Analysis of Dimensional Control in 3D Printing

by

Khalil Sardouk

Submitted to the Department of

Mechanical Engineering

in Partial Fulfillment of the Requirements

for the Degree of

BACHELOR OF SCIENCE

at the

MASSACHUSETTS INSTITUTE OF TECHNOLOGY

December 1993

Signature of Author

Department of Mechanical Engineering, December 20,1993

Certified by

Emanuel M. Sachs, Associate Professor

Thesis Supervisor

Accepted by

Peter Griffith

Chairman, Department Committee

Analysis of Dimensional Control in 3D Printing

by

Khalil M. Sardouk

Submitted to the Department of Mechanical Engineering on December 7,1993

in Partial fulfillment of the requirements for the

Degree of Bachelor of Since in the Mechanical Engineering.

ABSTRACT

In an effort to find out the deviations of printed ceramic parts on the newly developed 3D machine and the air force effect on the first drop of the binder stream, an experimental study was conducted. The errors that caused the deviation were molded as shrinkage errors, depend on the dimension of the parts, and additive errors, do not depend on the dimensions but on fixed parameters such as the actual lines widths.

Dimensions of ceramic parts were measured in the fast and slow axes of the machine. The binder was Nyacol 9950 collodial silica sol flowing at 1.3 ml/min., the layer thickness was 170μm, the line spacing was 175μm, and the powder was Norton aluminum oxide 30μm with a powder bed density of 35%. The printing variables were the citricity of the powder , the misting ratio, the direction of printing, and the firing temperatures. There were 6 experiments in the slow axis with different set of variables and 3 set of experiments in the fast axis with different set of variables. The measurements were then plotted and linearly fitted to determine the additive and shrinkage components for each of the experiments. A file was generated to detect the deviation of the first drop of the binder stream from the targeted position due to the air force effects.

The additive and shrinkage errors varied for each of the 9 experiments . The additive errors in the fast axis was of an average of 9.95±0.8 mills which is the diameter of a printed line. While the shrinkage in the fast and slow axis with the additive errors in the fast axis had no unique values to drive a good conclusions from. Moreover, it was concluded that the air drag force has a continuos effect on the binder stream. It has no effect on the dimensional deviation of parts, it only cause parts to be printed in different locations than their intended ones.

Thesis supervisor: Dr. Emanuel Sachs
Title: Associate Professor of Mechanical Engineering

Dedication

All the effort that I have put into this thesis and my four years of college, goes as a modest gift to my father and mother and my two beautiful sisters, Baria and Faten. They are every thing to me and I hope they will be always proud of me.

Acknowledgments

I would like to thank Professor Sachs for letting me work on the 3D project. I am grateful for his support and enthusiasm in teaching me research and lab work, the most important knowledge that I have gained in my undergraduate years.

Special thanks to Alain Curodeau and Jim Bradt for teaching me to use the software and machines, and congratulations for your Ph.Ds.

Thanks to Jain Charnnarong, Jim Serdy, and Dave Brancazio for making my thesis easy and interesting.

Finally I would like to thank Fred Coté for teaching me a lot about machining and making me a good machinist.

Table of Contents

List of figures

List of Tables

1. Introduction

1.1 Motivation

An ingenious idea in a rapidly growing industrial world is the development of the three dimensional printer. This machine eliminates current expensive, slow, and inflexible manufacturing techniques. 3D parts are used in industry either as molds or directly as prototype parts.

The 3D machine is still being researched and work is being done on its mechanism, software, electronics, and materials for parts. Moreover, the dimensions of the printed parts tend to deviate from file specifications. The errors that cause this deviation can be though of as having two components. One component dose not depend on the length of the sample and the other component is a function of the length. The first type is termed "additive" and the second type is termed "shrinkage".

Since the manufactured 3D parts are used for tooling or as direct prototypes, the accuracy is of extreme importance. The focus of this thesis is to find what causes the deviation of dimensions from their specified ones. The results of this study will be used to predict and reduce these errors.

1.2 Three Dimensional Printing

Three dimensional printing is the process of manufacturing complex shapes directly from a computer model, without the need for tooling. It can be used to fabricate parts made of ceramics, metals, ceramic-metal, or polymeric material. The final objective of the machine is to produce parts that will be used in tooling or as direct prototypes.

Three dimensional printing utilizes a layered printing format. (Figure 1.1). The data for each layer is obtained by applying a slicing algorithm to the computer model. Each layer is printed on a bed of powder deposited on the top of a piston and cylinder. The powder is joined at selected locations by means of ink jetted binder. The piston and the layer are then lowered for another powder spread. Subsequent layers are printed in the same sequence as the preceding one. This layering process is repeated until the part is fully manufactured. Then the piston moves all the way up and the part is removed and heat treated to solidify it.

The printed part could be manufactured with different variables: Powder material, amount of water vapor, the direction of printing, the firing temperature, the binder flow rate, and layers thicknesses. As mentioned earlier, the powder used could be ceramic, metal, metal-ceramic, or polymeric. while the part is being printed, it could be either misted or not by means of water vapor directed at the powder bed. The binder stream could be released in one fast axis direction, for example releasing the binder from right to left only, or the binder could be released in both direction of the fast axis, from left to right and right to left. The first kind of binder release is called one directional printing and the second is called two directional printing. Finally, the printed part could be heat treated by either baking under low temperatures for long hours or by firing it at high temperatures such as the conventional ones of 750°C and 900°C.

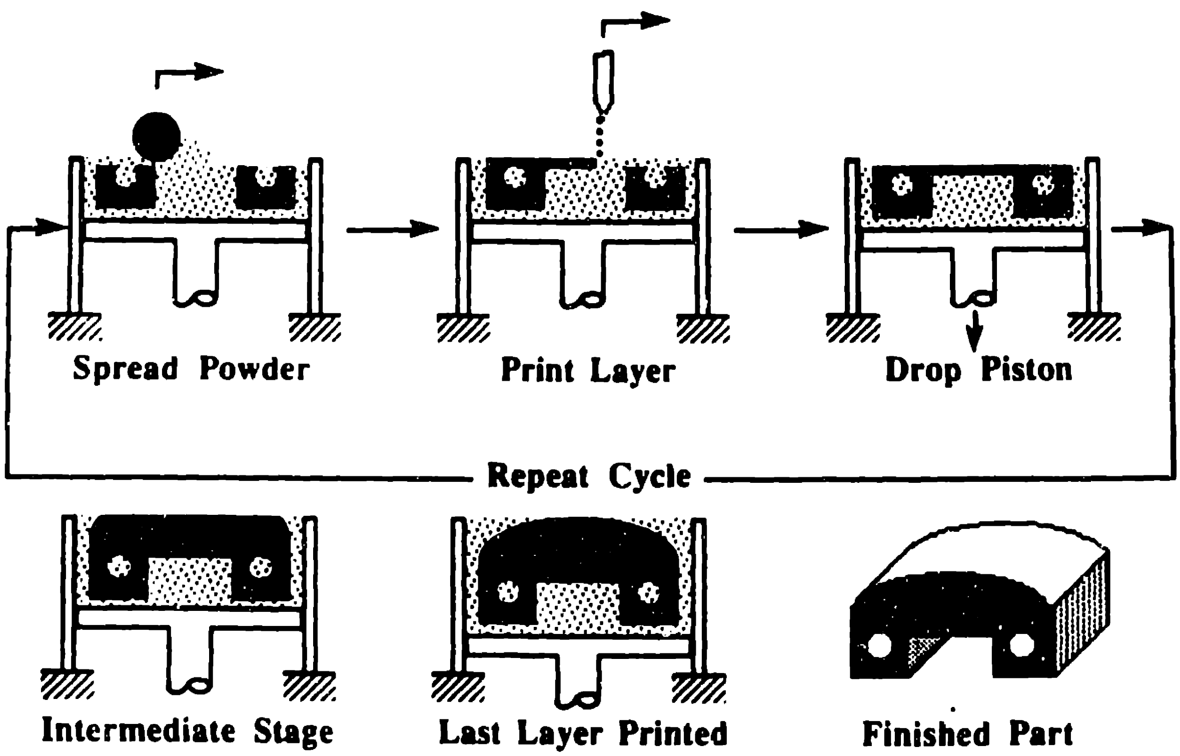

Figure 1.1: Sequence of operation in the 3D printing process

2. Experimental Procedure

2.1 Apparatus

2.1.1 The 3D Machine

The 3D machine, Figure 2.1, was used to print the parts for this study. A computer aided design , CAD, software is used to generate a data file which instructs the 3D machine to print a cross section of the part drawing layer by layer. The fabrication of the part is done by means of spreading powder on a vertically movable piston, the Z axis, then solidifying the powder by reacting it with a binder. The binder is jetted through a printhead that moves along the "fast axis" and eventually solidifies the powder into a printed line. The jet is released only to print the sections of the line instructed by the part's file. Then the printhead traverses the layer in the "slow axis" direction to print an adjacent line. When the cross section of a part is printed on a layer, the piston moves vertically downwards and new powder is spread following the same process as the preceding layer. The part is fabricated when all the layers are printed. Finally, the piston moves all the way upward on the Z-axis so that the part can be removed. The part is heat treated and then dusted off to remove any loose powder.

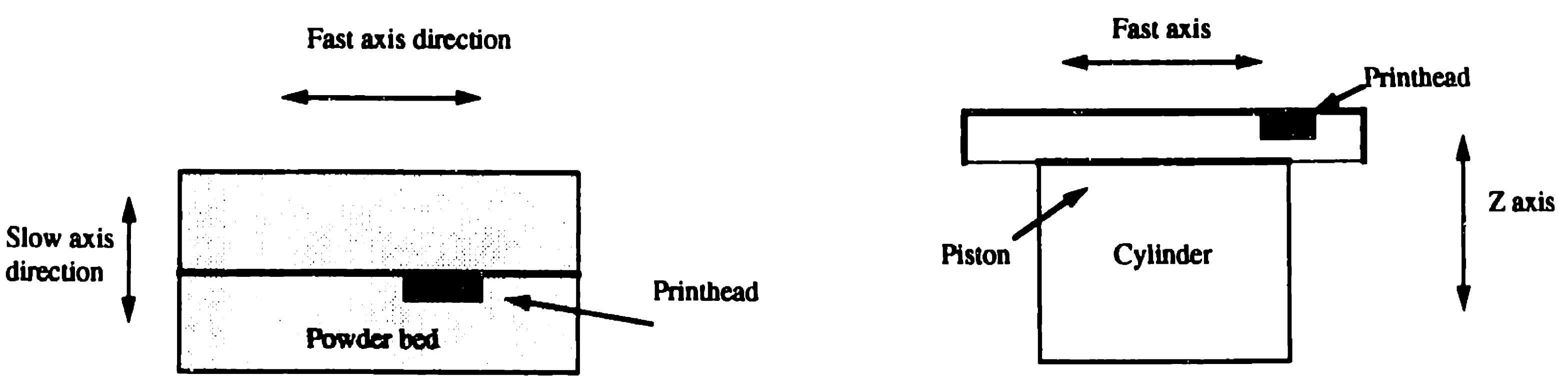

Figure 2.1 : The 3D machine

2.1.2 Measuring Tools

Since the research focuses mainly on having as accurate measurements as possible, measuring technique was thoroughly addressed. Several measuring techniques were considered. One was the use of a super micrometer, but because it was old and may not have been accurate, it was ruled out. Another possibility was the use of a sensitive probe screwed into a digital milling machine and calibrated to read a desired height. The calibration of the milling machine would be used to measure the positive or negative offset of a part's height from the already calibrated one. Although this measuring method has 0.00005" of accuracy it would measure local heights due to the fact that the head of the probe is small and that the printed parts have an irregular surface texture, therefore, it was also ruled out as a useful measuring instrument. Moreover, optical measurements were not acceptable since visual measurements would measure the distances only between the high ends of the surfaces.

The measuring technique finally used was a pair of calipers. The calipers were digital Brown & Sharpe with an accuracy of 0.0005". The calipers were the best way to measure the testing parts because of the parts' uneven surface. The flat wide edges of the caliper ignored the irregularities and avoided local measurements of the part. It averaged out the irregularities and provided more usable measurements. Long parts were clamped onto a flat table and then measured with the calipers in order to prevent breakage.

Moreover, the SEM machine of Cambridge Stereoscan was used to see the micro-structure of the printed lines and layers.

2.2 Materials

2.2.1 Powders

The powder used was Norton aluminum oxide 30 μm of Norton Corporation, Northampton, Massachusetts. To make the powder acidic, a 0.2% by volume citric acid was added.

2.2.2 Binder

The binder used in this study was NYCOL 9950 Colloidal Silica Sol manufactured by PQ Corporation of Ashland, Massachusetts.

2.3 Printing In the Slow Axis

2.3.1 Dimensions of the Printed Parts

In order to determine the shrinkage and additive errors in the slow axis, a file was generated, *fast20bars*, using Make3DP software programmed by Alain Curodeau. This software enabled us to specify dimensions in the slow axis with exact confidence. The parts were bars of cross sectional areas of 0.372" in the fast axis and 0.3748" in the Z axis. The lengths of the bars in the slow axis were determined by specifying within the file the position of the centerline of the outermost scans of the fast axis which define the printed component. These centerline to centerline dimensions were: 0.372", 0.7441", 1.998", and 3.9961". Naturally, the actual part boundary extends beyond the centerline of printing and this factor is one contribution to the additive component of the error. The file was named *fast20bars* and enabled us to print five bars of each length in order to examine the statistical significance of the results. Figure 2.2 shows a top view of the bars printed in the slow axis.

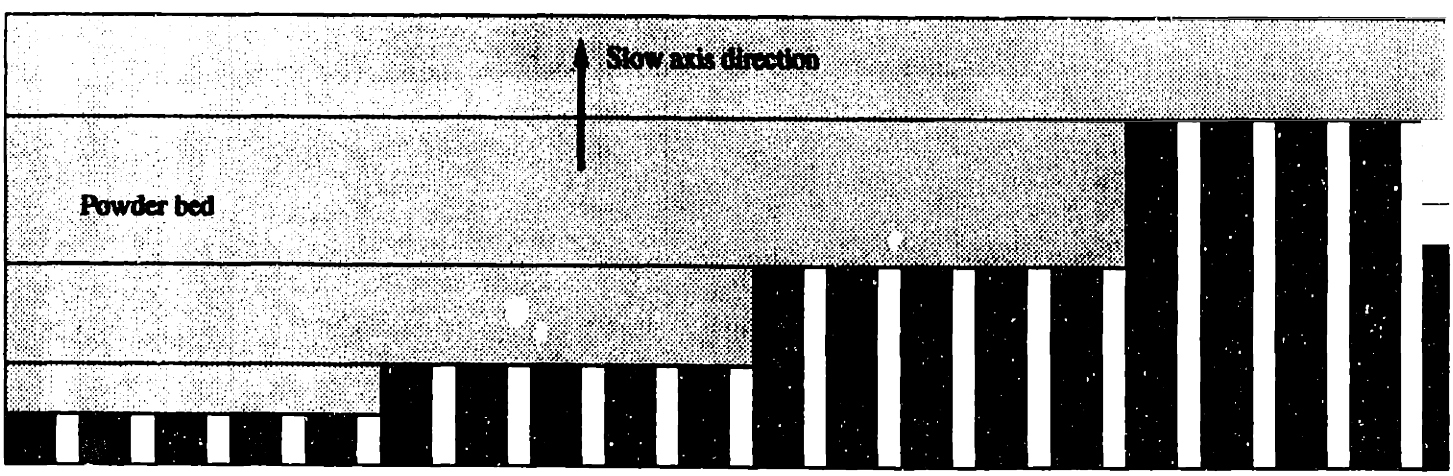

Figure 2.2: A top view of printed bars in the slow axis, figure is not scaled.

2.3.2 Printing Experiments and their Variables

The *fast20bars* file was used to print under different combinations of four variables. Table 2.1 shows the experiment number and the variables under which it was printed. For all six experiments, the line spacing was 175μm, all layers were 170μm thick, and the binder flow rate was targeted to 1.3 ml/min.

Table 2.1: The Experiment number and their variables used to print bars in the slow axis

Experiment #	Powder	Misted	Firing Temp.°C	Printing Direc.
1	Citric	Yes	750	2 Way
2	Citric	No	750	2 Way
3	Non-Citric	Yes	750	2 Way
4	Non-Citric	No	750	2 Way
5	Citric	Yes	900	2 Way
6	Non-Citric	No	900	2 Way

The parts used in experiments 5&6 were the same parts as those used in experiments 1&2 respectively. The only difference is that they were re-fired to 900°C for one hour.

2.4 Printing In the Fast Axis

2.4.1 Dimensions of Printed Parts

A file was generated to print bars in the fast axis using Pro-Engineer. The bars had cross sectional area of 0.375" in both the slow and Z axis. Their widths in the fast axis were the distance between the far ends of the lines which had dimensions of 0.5", 1.00", 2.00", 4.00", and 8.00". The actual widths of the parts is larger taking into account the sizes of the bounded materials, non the less the additive error will take it into account. The file was named *testbar7* and printed bars as shown in Figure 2.3. The *testbar7* was modified to *testbar4* that does not print central bars in order to save time.

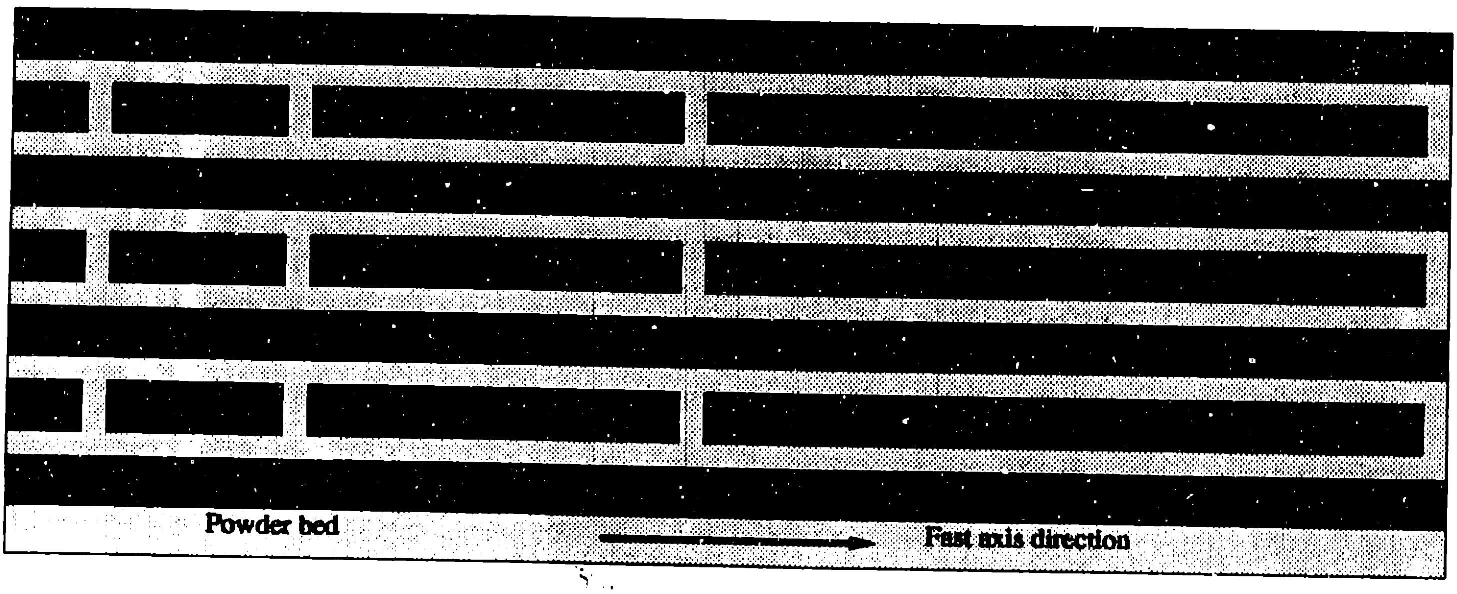

Figure 2.3: A top view of printed bars in the fast axis, figure is not scaled.

2.4.2 Printing Experiments and their Variables

Testbar7 was used to print experiment 2, while *testbar4* was used to print experiments 1&3. Table 2.2 shows the experiment number and the variables under which it was printed. For all the experiments the line spacing was 175µm, all layers were 170µm in thicknesses, and the binder flow rate was targeted to 1.3 ml/min.

Table 2.2: Experiment number and their variables used to print bars in the fast axis

Experiment #	Powder	Misted	Firing Temp.°C	Printing Direc.
1	Citric	Yes	900	2 Way
2	Citric	No	900	2 Way
3	Citric	Yes	900	2 Way

2.5 Calculating the Drag Force Effect

Hypothetically there is an air-drag force on the first drop of the released binder stream. This force causes the first drop to fall at a further distance than the targeted location (Figure 2.4a). In order to determine the distance error that is caused, a file named *Drag-Error.3dp* was generated using Make3DP and printed 112 one directional lines as follows. There were two sets of lines. Set A are those lines printed from position 0 to 1000 µm. The other set, B, are lines printed from position 1000 to 2000 µm. Lines were printed alternating from each set with a space of 350 µm in-between each line. (Figure 2.4b).

Due to air drag force the first drops in lines A should fall past 0 µm position and the same is so for the first drops of lines B which should fall past position 1000. On the other hand, the last drops of all the lines in both sets should fall at their targeted positions, that is, 1000 µm and 2000 µm for lines A&B, respectively, since the air drag force is minimized. Connecting an imaginary line between the end of the lines of set A and another imaginary line for the beginnings of the lines of set B, one could determine the shift in locations for the beginnings of lines in set B from what was targeted. This shift is cased by air drag force and could be measured using an SEM machine. (Figure 2.4c)

The layer that consist of lines As&Bs was printed on five preceding layers so that the lines would not brake off easily. The six layers were printed on a large SEM stub. A washer was silver glued to the stub to get a streng base for the printed layers. (Figure 2.4d). File *Drag-Error.3dp* enabled us to print the specimens on four different powder bed locations. (Figure 2.4e). The four specimens were printed using citric ceramic powder and one set was misted while the other set was not misted. The two sets of misted and not misted specimens were backed at 300°C, to avoid melting the stubs themselves, for 24 hours. Then the two sets were gold plated and experimented under an SEM machine.

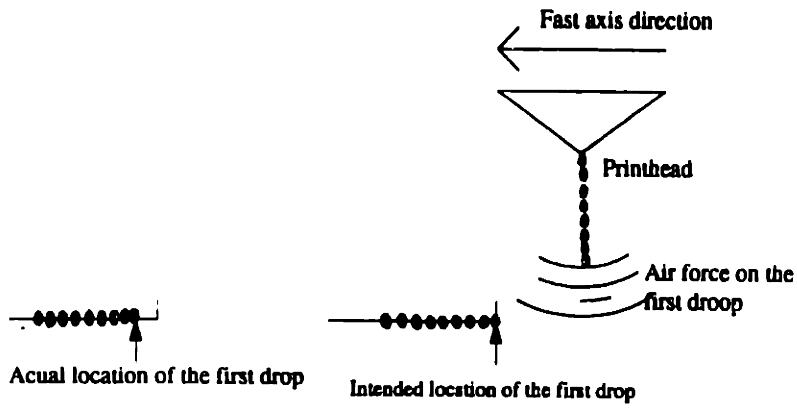

Figure 2.4a: The effect of the air drag force on the first released binder drop.

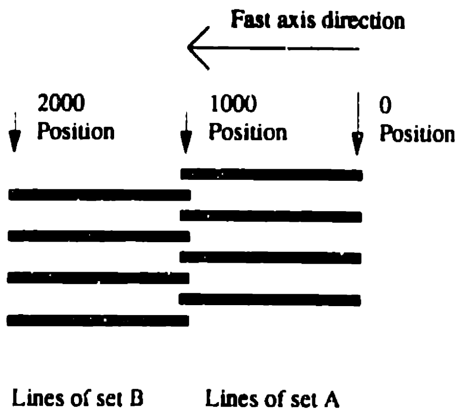

Figure 2.4b: A sample of A&B printed lines.

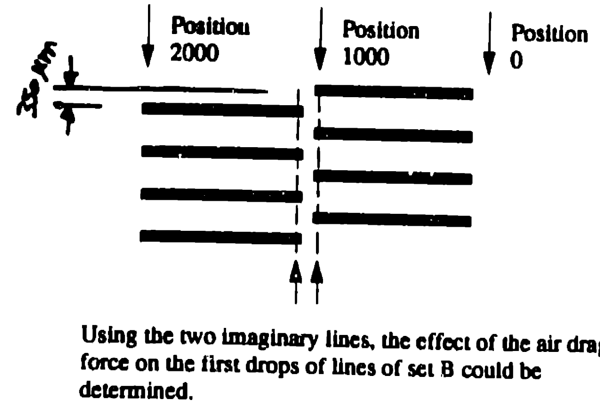

Figure 2.4c: The shift of the beginning of the lines from 0&1000 μm positions,

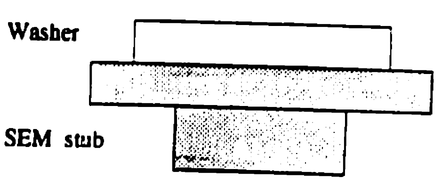

Figure 2.4d: The SEM stubs used to print the specimens..

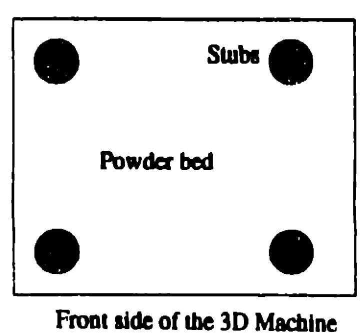

Figure 2.4e: The locations of the stubs on the machine.

1 Results

1.1 Slow Axis Measuring Results

For each of the six experiments, the measured lengths in the slow axis were plotted on the x-axis and the deviation of the measured length from the intended ones, what we had specified in the *fast20bars* file, were plotted on the y-axis. Graphs were linearly fitted. Even though a linear fit is not the best fit, it gives the graphs significant values by looking at the line slope and on the intersection of the line with the Y axis. The reason for saying that a linear fit is not the best solution is due to the fact that the collected data do not pass through some of their error bars. Such thing would make a linear fitting an unconfident fitting and a higher degree fitting might be advisable. For example, Figure 3.1 shows a linear fitting for experiment 1 of table 2.1 for a citric misted 2Dir. 750 °C parts. The figure shows by linear fitting the results, measurements, we would miss three out of the four error bars of the measurements. The error bars represent the ± the standard deviation of the measurements divided by the sq. root of the number of measurements taken. The results for experiment 1 though 6 are shown in figures 3.2 to 3.7 respectively. The significance of a linear fit is that the slope represents the shrinkage since it depends on the dimensions of the parts, and the intersection of the line with the Y axis is the magnitude of the additive error since it is present even for a 0 part dimension. Large number of parts in the citric not misted two directional 750° C experiment, experiment 2, got broken easily. The data of the measurements taken are tabulated in appendix A.

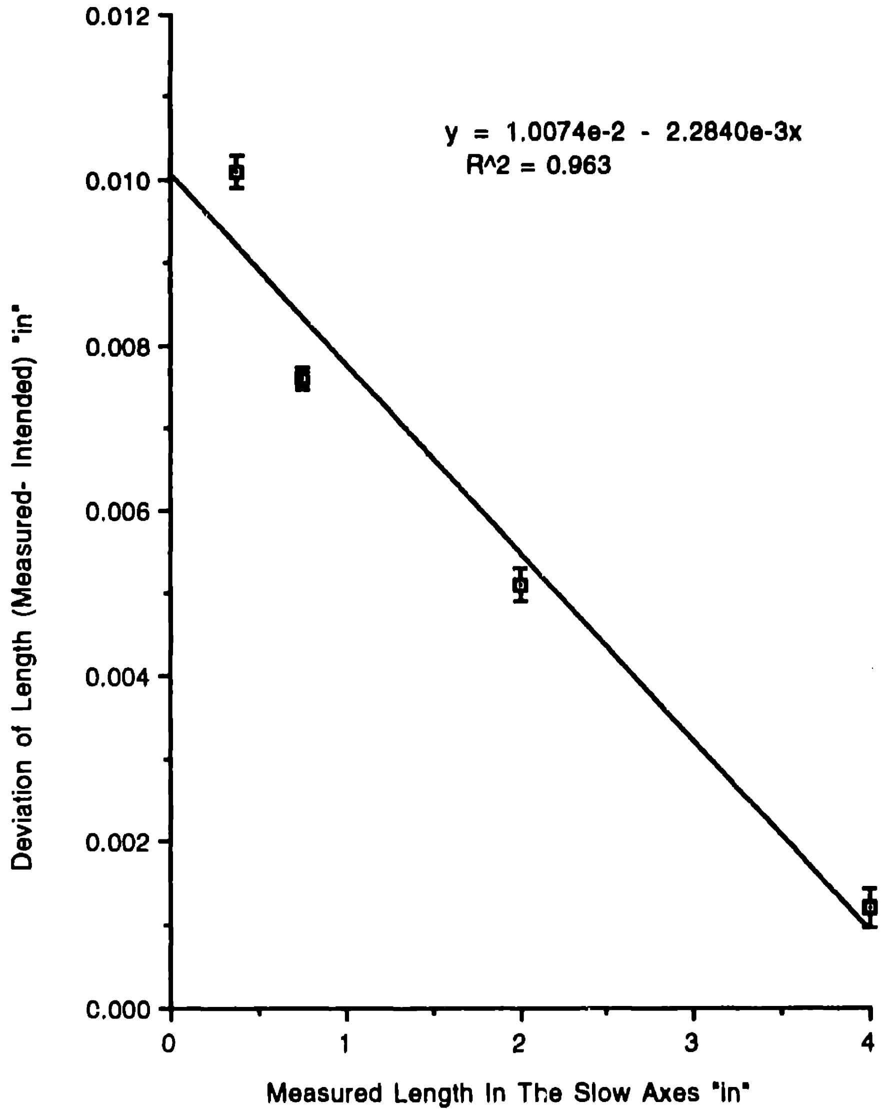

Figure 3.1: Results for citric misted 2Dir.750°C, Experiment 2 of table 2.2. linearly fitting experiment # 2 results in missing the error bars the measurements. Error bars are the ± standard deviation of the measurements for a part divided by the sq. root of the number of measurements taken on that part, 5 measurements.

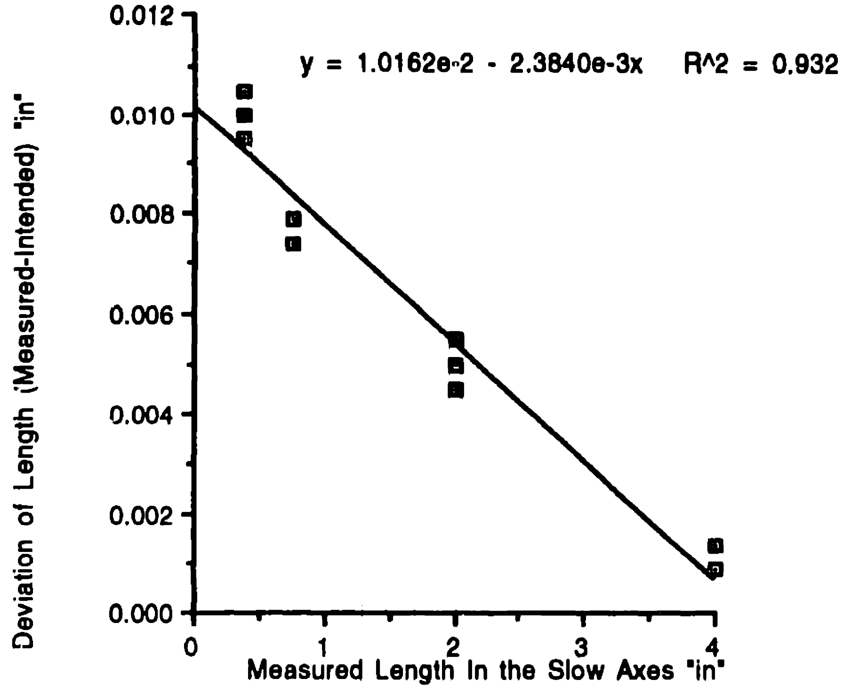

Figure 3.2: Results for citric misted 2Dir.750°C parts, Experiment 1 in table 2.1. The slope of the line shows shrinkage, -0.023%, while the intersection shows the additive error, 10.1 mills.

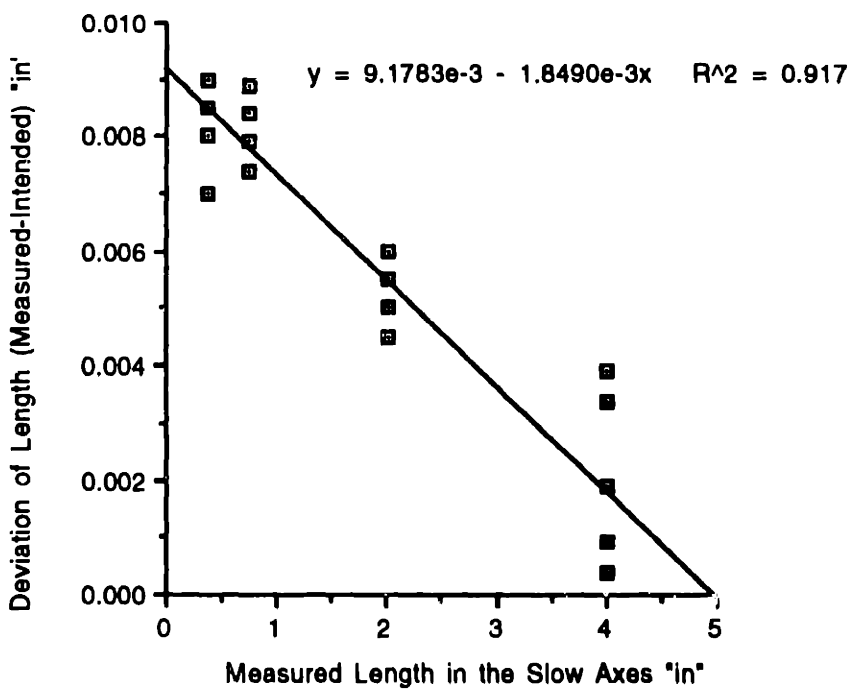

Figure 3.3: Results for citric not misted 2Dir.750°C parts, Experiment 2 in table 2.1. The slope of the line shows shrinkage, -0.018%, while the intersection shows the additive error, 9.17 mills .

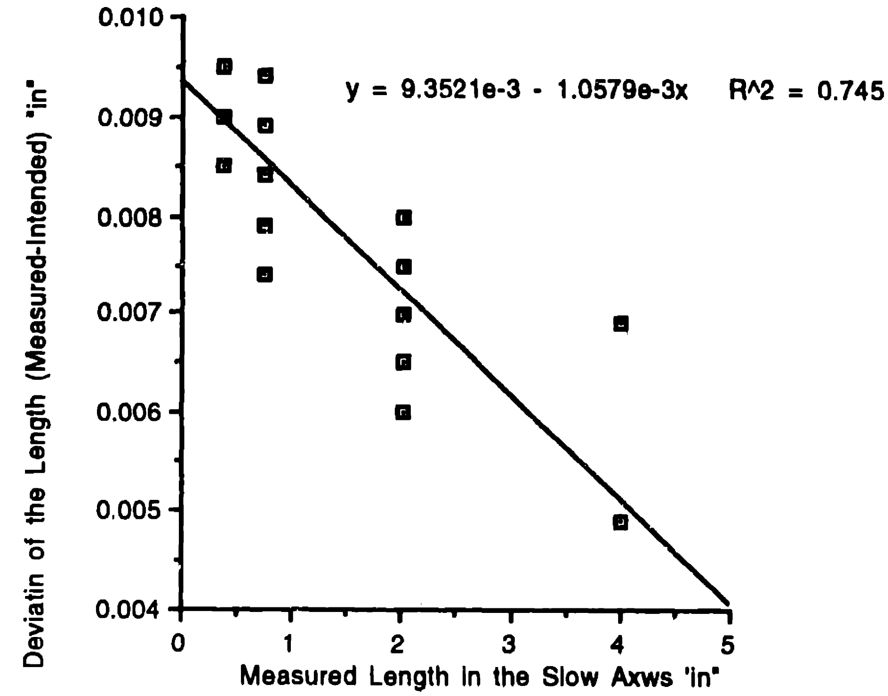

Figure 3.4: Results for citric misted 2Dir.750°C parts, Experiment 3 in table 2.1. The slope of the line shows shrinkage, -0.01%, while the intersection shows the additive error, 9.35 mills .

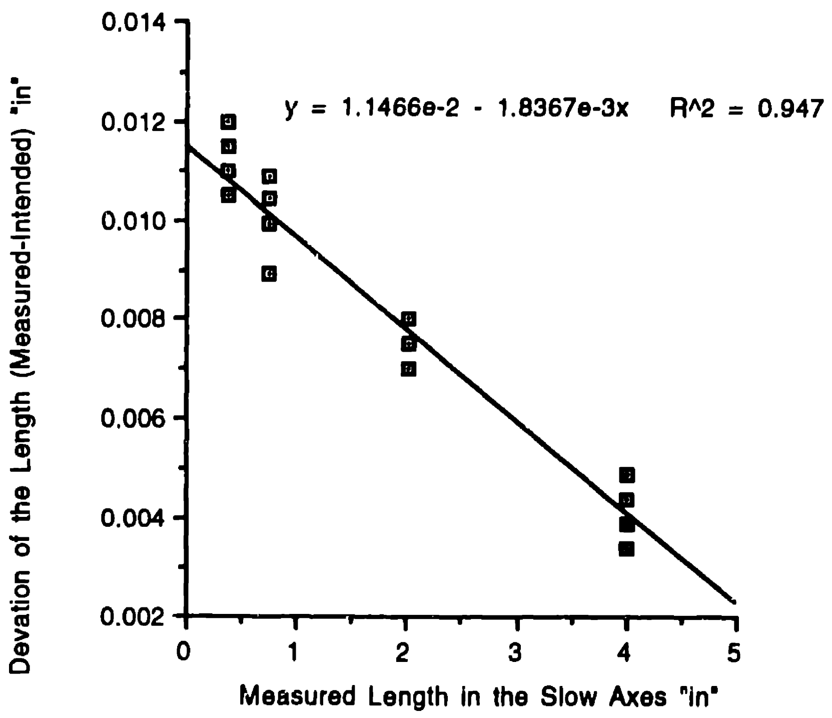

Figure 3.5: Results for citric misted 2Dir.750°C parts, Experiment 4 in table 2.1. The slope of the line shows shrinkage, -0.01%, while the intersection shows the additive error, 9.35 mills.

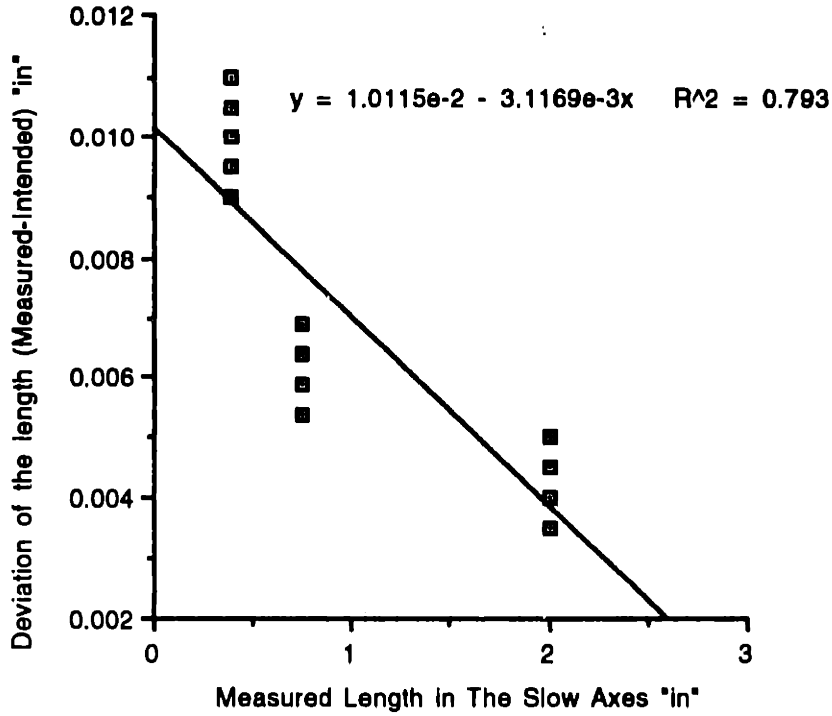

Figure 3.6: Results for citric misted 2Dir.900°C parts, Experiment 5 in table 2.1. The slope of the line shows shrinkage, -0.031%, while the intersection shows the additive error, 10.1 mills .

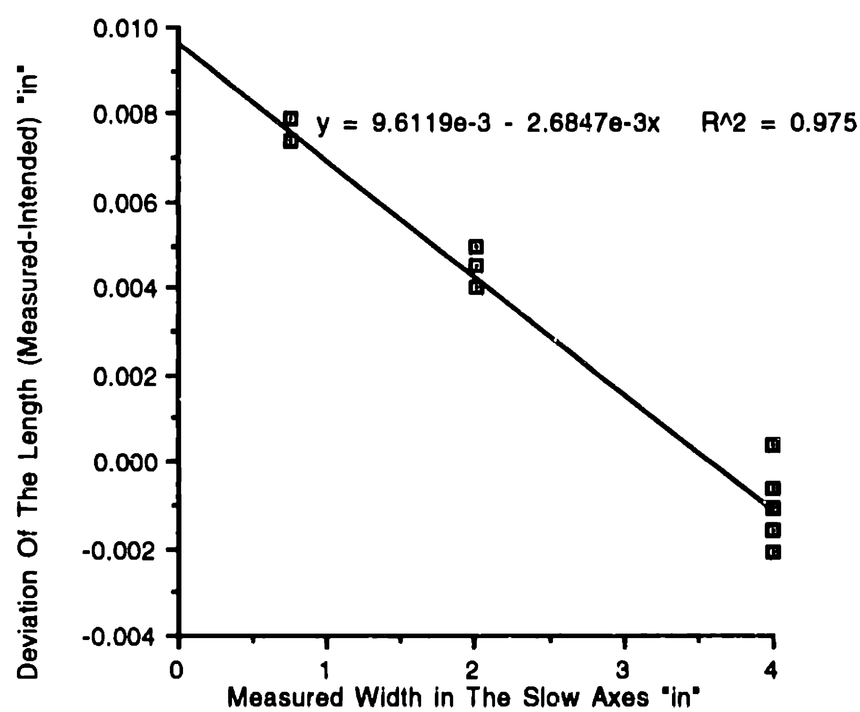

Figure 3.7: Results for citric not misted 2Dir.900°C parts, Experiment 6 in table 2.1. The slope of the line shows shrinkage, -0.026% , while the intersection shows the additive error, 9.61 mills.

1.2 Fast Axis Measuring Results

The printed horizontal bars were separated into three sections on the powder bed. A front, center, and back sections. The back bars are the ones printed at the far end of the machine, parts printed first. The front bars are the ones printed at the front of the machine, parts printed last. For each section of the three experiments, the measured dimensions in the fast axis, call the measured widths, were plotted on the X-axis while the difference between the measured widths from the intended ones were plotted on the Y-axis. Figure 3.8 through 3.14 shows the front, center, and back results for experiment 1 through 3 in table 2.2. The results were linear fit. The slope shows the shrinkage value while the intersection of the line with the Y axis represents the additive error value. Experiment 1,3 used *testbar4, while* experiment 2 used *testbar7* to printed. The data of the measurements of experiments 1&2&3 of table 2.2 are tabulated in appendix B.

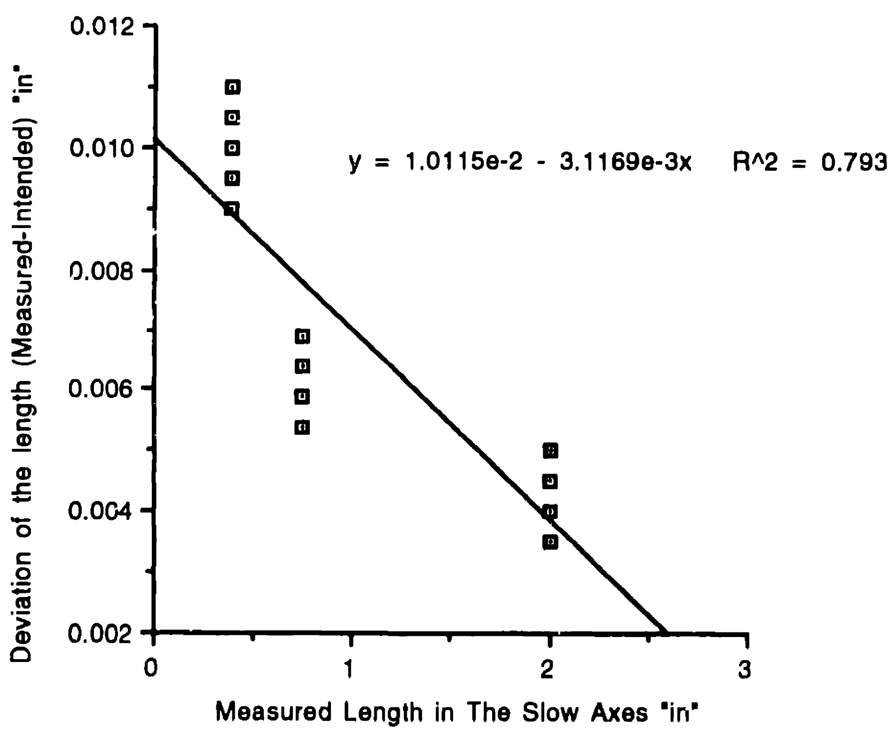

Figure 3.8: Results for the front bars of the citric misted 2Dir.900°C, experiment 1 in table 2.2. The shrinkage error was -0.031%, while the additive error was 10.1 mills.

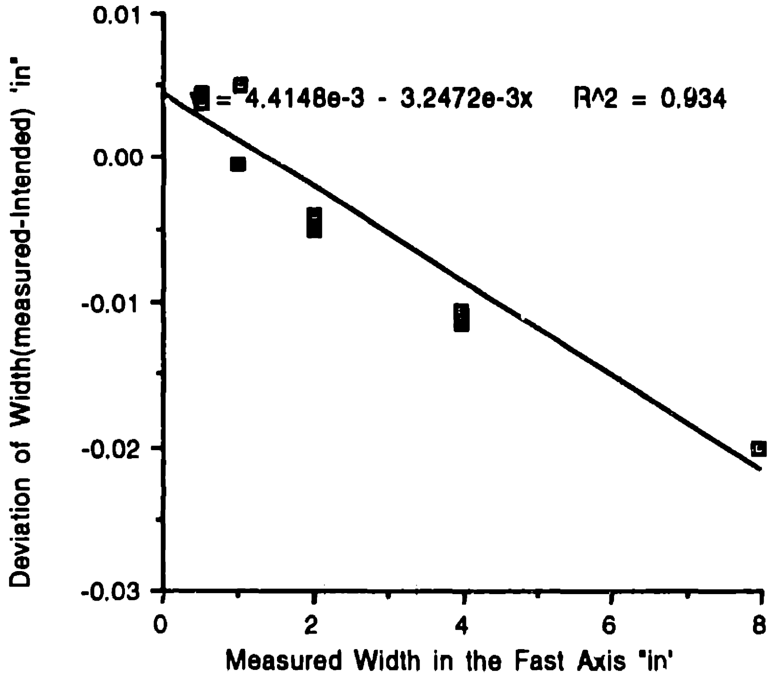

Figure 3.9: Results for the back bars of the citric misted 2Dir.900°C, experiment 1 in table 2.2. The shrinkage error was -0.033%, while the additive error was 4.4 mills.

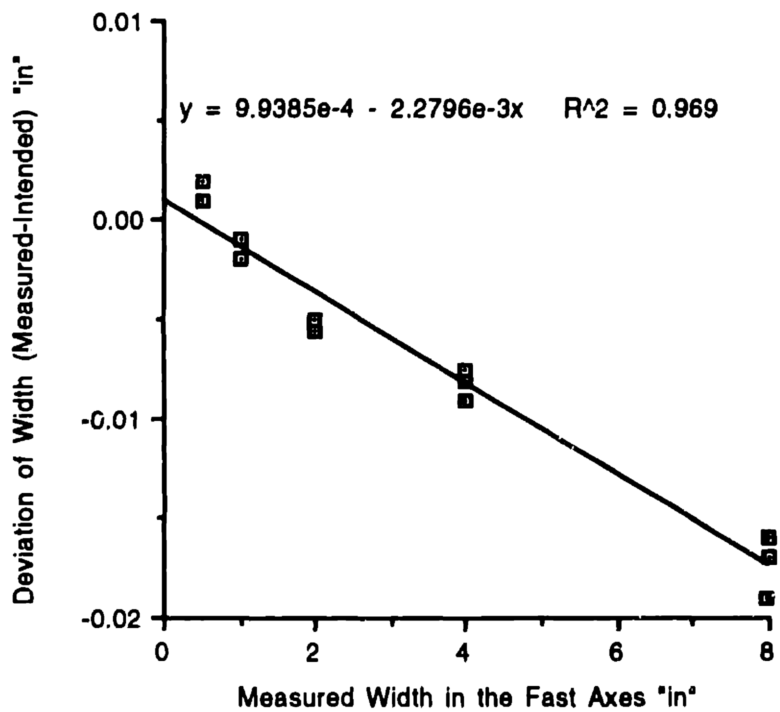

Figure 3.10: Results for the front bars of the citric not misted 2Dir.900°C, experiment 2 in table 2.2. The shrinkage error was- 0.022%, while the additive error was 0.99 mills.

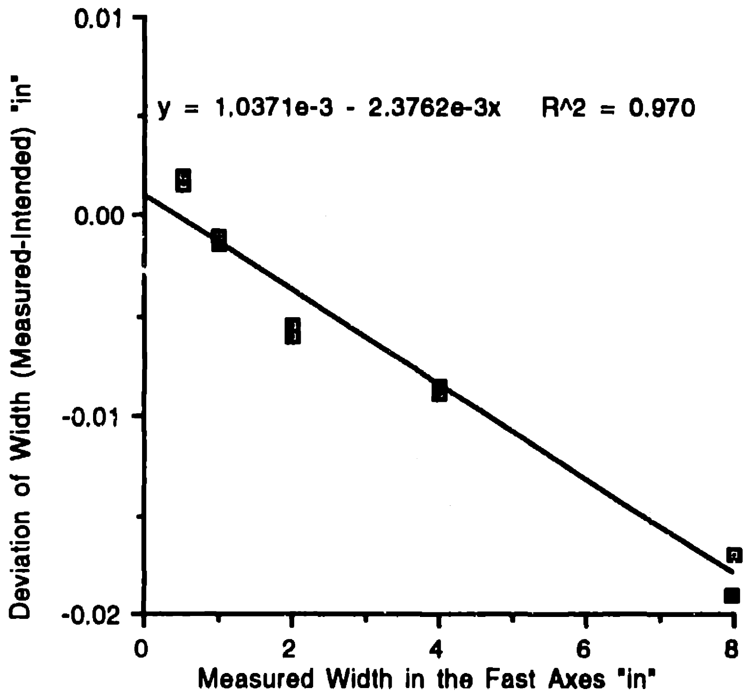

Figure 3.11: Results for the center bars of the citric not misted 2Dir.900°C, experiment 2in table 2.2. The shrinkage error was -0.023%, while the additive error was 1.0 mills.

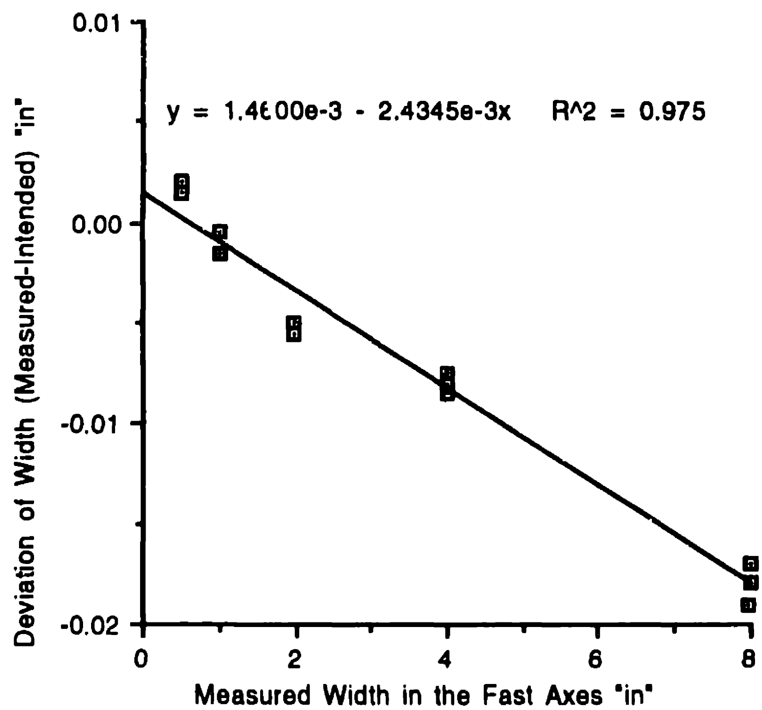

Figure 3.12: Results for the back bars of the citric not misted 2Dir.900°C, experiment 1 in table 2.2. The shrinkage error was -0.024%, while the additive error was 1.4 mills.

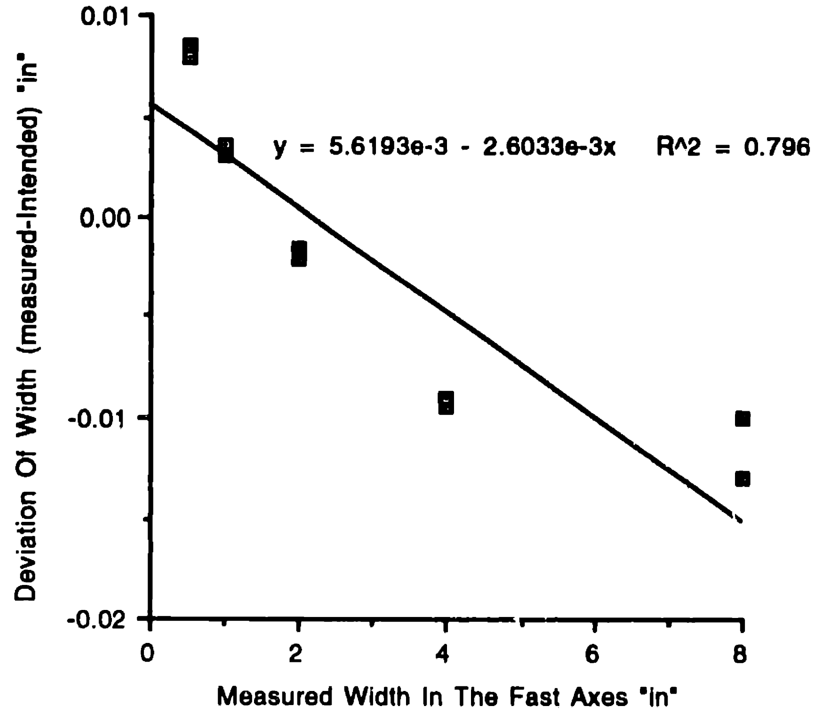

Figure 3.13: Results for the front bars of the citric misted 1 Dir.900°C, experiment 3 in table 2.2. The shrinkage error was- 0.026, while the additive error was 5.6 mills.

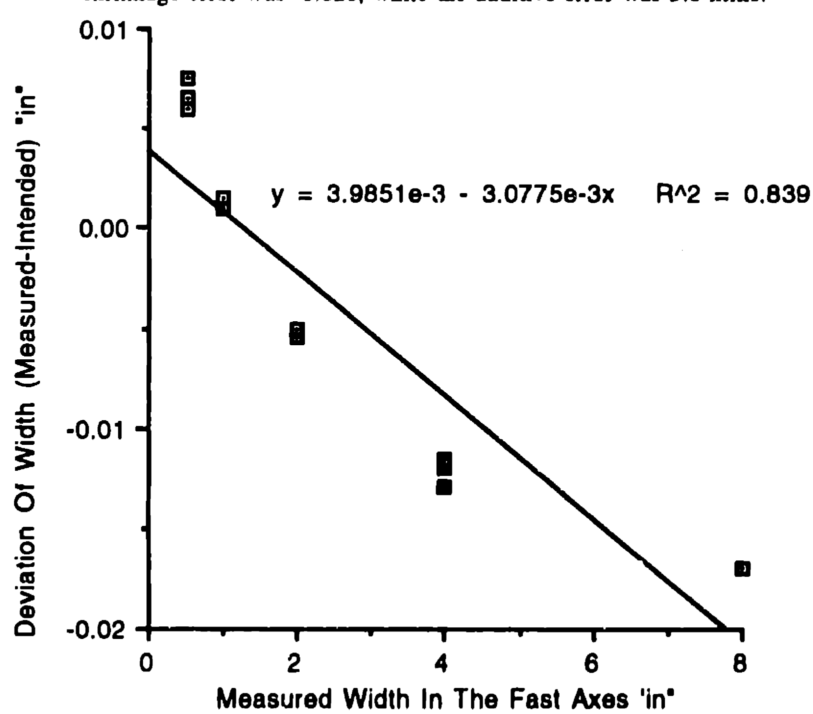

Figure 3.14: Results for the back bars of the citric misted 1Dir.900°C, experiment 3in table 2.2. The shrinkage error was -0.03%, while the additive error was 3.9 mills.

3.3 The Air Drag Force

The *Drag-Error.3dp* file was used to print the four sets of the testing stubs under the citric, misted and not misted conditions. Unfortunately the 350 μm chosen separation between the lines was small and hard to obtain useful information from. Figure 3.15 Shows an SEM Sony pictures of a front right not misted printed lines.

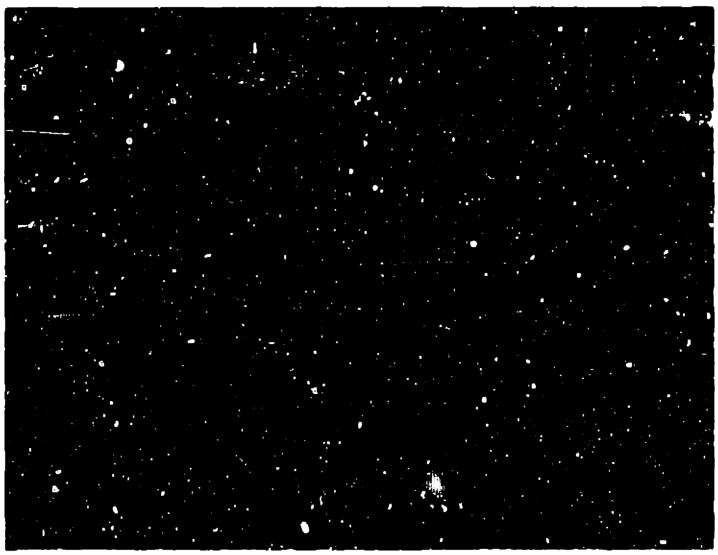

Figure 3.15 : An SEM photo for a front right not misted specimen using *Drag-Error.3dp* file. As it is noted the lines tend to merge at the sides.

Therefore, in order to obtain a better results, the *Drag-Error.3dp* file was modified to avoid the interference of the lines by increasing the separation between a line from set A and a line from set B from 350 μm to 700 μm. The results were surprising. The SEM pictures did not show any kind of shift of the beginning of lines of set B from the ends of the lines of set A. (Figure 3.16). As the SEM picture shows, the end of the lines overlapped with the beginnings of the other set of lines. The overlap is due to the fact that the lines of set A&B in the generated files are one dimensional but in reality the printed lines are three dimensional. This over lap ranges from 80 μm to 100 μm, which is around half of the diameter of a printed line, indicates that the last drop of lines A fell in its intended position the same for the first drops of line set A.

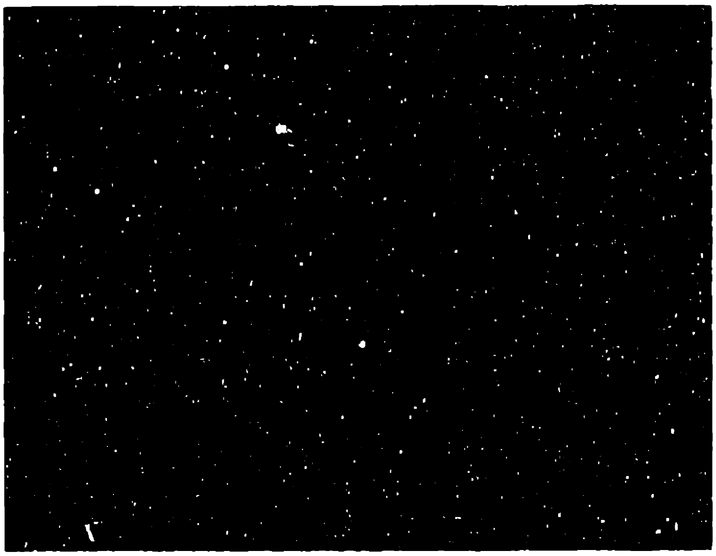

Figure 3.16 : An SEM photo for one of the specimens fusing an *Drag-Erro.3dp* file. As it is noted the lines fall in their intended positions and the over lap is due to actual drop size.

4 Conclusions and Discussion

4.1 Conclusions for the Slow and Fast Axis Experiments.

Table 4.1 and 4.2 sows a summary of the results for the slow and fast experiments respectively.

Table 4.1: A summary of the results of the shrinkage and additive errors for the slow axis experiments.

Experiment # and its Description	Additive error ' 0.001" '	Shrinkage " % "
1: Citric Misted 2Dir 750 °C parts	10.1	0.24
2: Citric Not misted 2Dir 750 °C parts	9.17	0.18
3: Non citric Misted 2Dir 750°C parts	9.35	0.1
4: Non citric Not misted 2Dir 750 °C parts	11.4	0.18
5: Citric Misted 2Dir 900°C parts	10.1	0.3
6: Citric Not misted 2Dir 900°C parts	9.6	0.27

Table 4.2: A summery of the results of the shrinkage and additive errors for the slow axis experiments.

Experiment	Front		Center		Back	
	Additive	Shrinkage	Additive	Shrinkage	Additive	Shrinkage
1: Citric, Misted 2Dir 900	10.1mills	0.3%	-		4.4 mills	0.32%
2:Citric Not misted 2Dir 900	0.1 mills	0.22%	1 mills	0.023%	1.4 mills	0.24%
3: Citric Misted 1 Dir 900	5.6 mills	0.26%	-		3.9 mills	0.3%

Several conclusions may be drawn from table 4.1 and 4.2

- The average additive error for the slow axis experiments was 9.95±0.8" mills. This is very important result since the average width if a printed line is 9.5 mills. Therefore, the additive error contribution is solely due to half the width of a printed line on one side plus another half of that line on the other side of the parts.
- It was supposed that the shrinkage be less for not misted parts while fixing other parameters. But that is not the case since some parts shrunk less when they were misted, experiment 3 & 4 table 4.1. Parts shrunk less in the misted case, 0.1 %, than in the not misted case, 0.18%
- The additive error in the fast axis varied in a very wide range. It is hard to conclude any good reasoning for this variation.

- It has been noted that some parts printed in the fast axis have different measured dimensions from one section to another. Therefore in order to see if there is a difference among the front, center, and back parts for each of the 0.5", 1.0", 2.0", 4.0", and 8.0" parts, graphs were plotted showing the average of the measurements for a single part with its error bars. The error bars represent ± the standard deviation of the part's measurements divided by the sq. root of the number of the measurements. If error bars for any two sections overlap, we can conclude that their is no difference between the two readings. Figures 4.1 through 4.15 are the comparisons of the sections for experiments 1, 2, and 3, respectively.

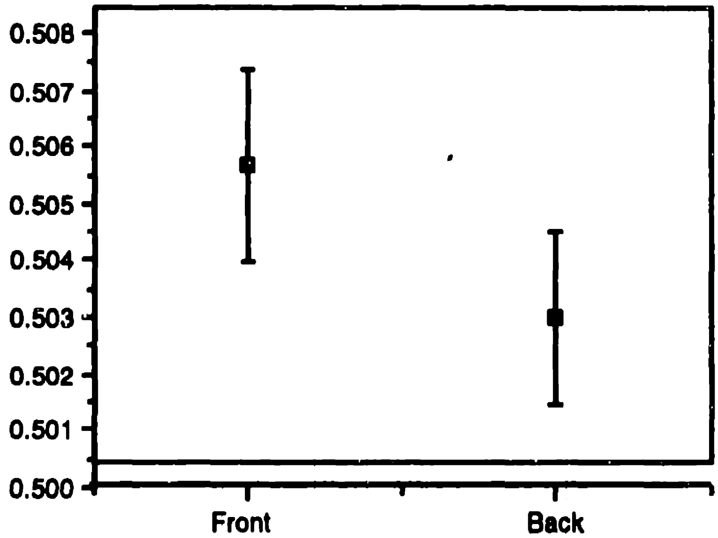

Figure 4.1: Experiment 1 in table 2.2: Comparison between the front and back measured widths for the 0.5" part using citric misted 2Dir. 900°C variables, . The points represent the average width. Error bars represent the standard deviation of the measurements divided by the sq. root of the number of measurements, 15 measurements.

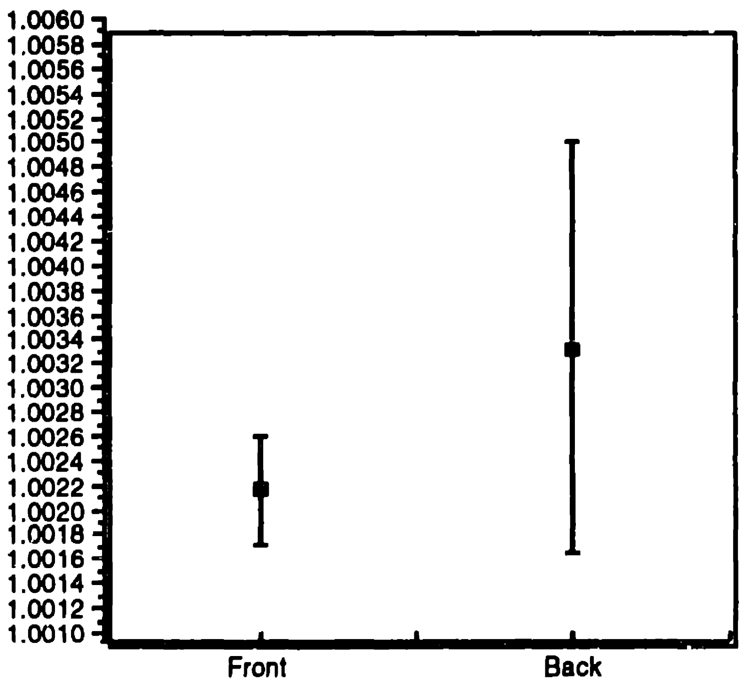

Figure 4.2: Experiment 1 in table 2.2.: Comparison between the front and back measured widths fcr the 1.0" part using citric misted 2Dir. 900°C variables, The points represents the average width,. Error bars represent the standard deviation of the measurements divided by the sq. root of the number of measurements, 15 measurements.

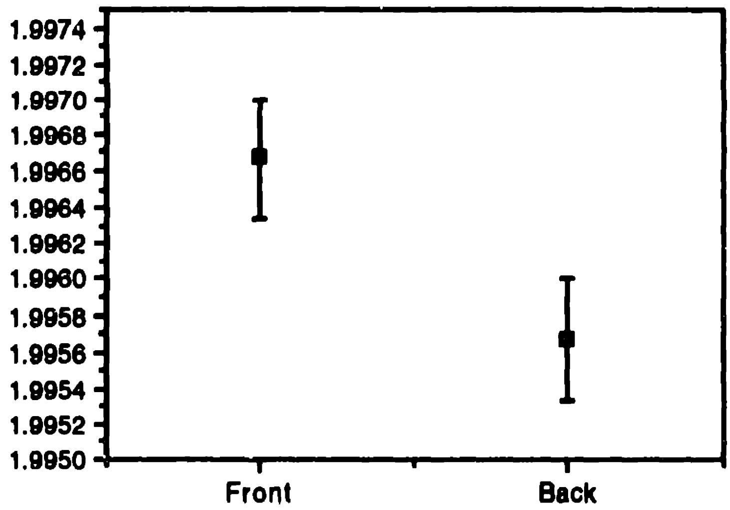

Figure 4.3: Experiment 1 in table 2.2: Comparison between the front and back measured widths for the 2.0" part using citric misted 2Dir. 900°C variables, . The points represents the average width. Error bars represent the standard deviation of the measurements divided by the sq. root of the number of measurements, 15 measurements.

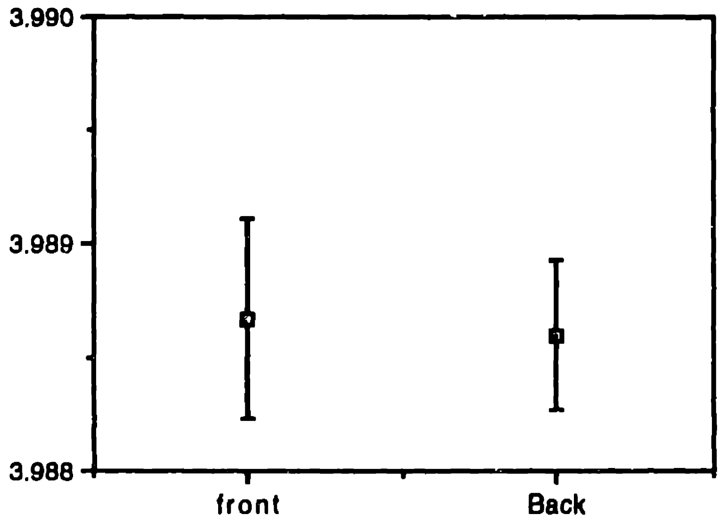

Figure 4.4: Experiment 1 in table 2.2: Comparison between the front and back measured widths for the 4.0" part using citric misted 2Dir. 900°C variables, The points represents the average width,. Error bars represent the standard deviation of the measurements divided by the sq. root of the number of measurements, 15 measurements.

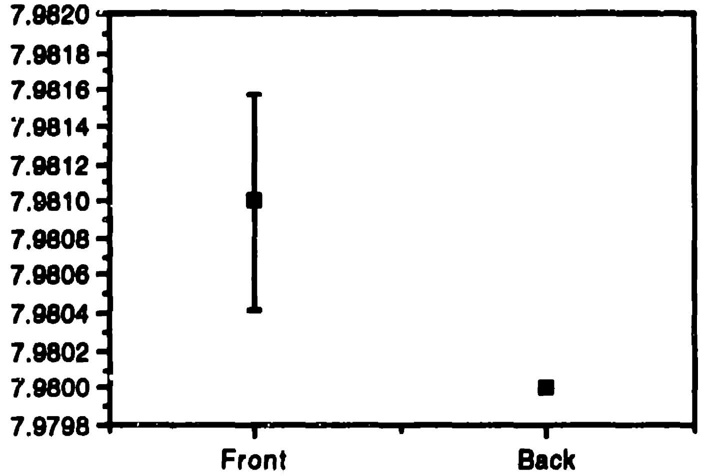

Figure 4.5: Experiment 2 in table 2.2.; Comparison between the front and back measured widths for the 8.0" part using citric misted 2Dir. 900°C variables, The points represents the average width,. Error bars represent he standard deviation of the measurements divided by the sq. root of the number of measurements, 15 measurements.

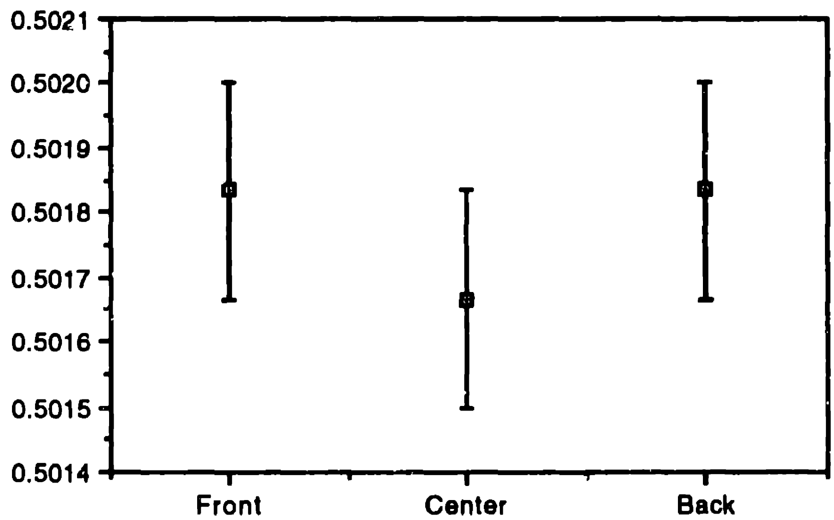

Figure 4.6: Experiment 2 in table 2.2: Comparison between the front, center, and back measured widths for the 0.5" part using citric not misted 2Dir. 900°C variables, The points represents the average width,. Error bars represent the standard deviation of the measurements divided by the sq. root of the number of measurements, 15 measurements.

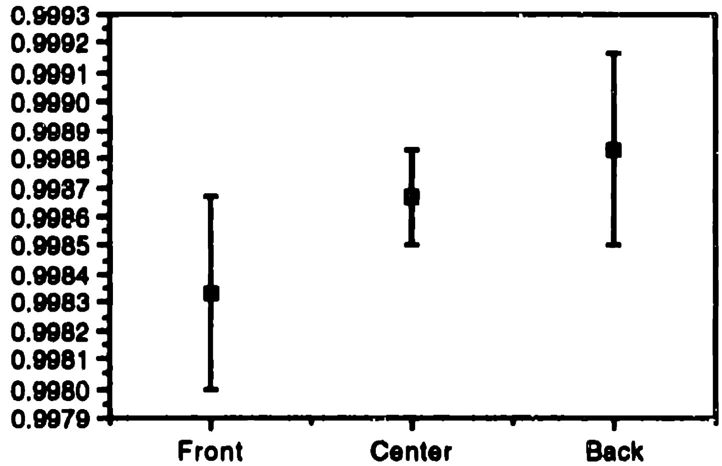

Figure 4.7: Experiment 2 in table 2.2 : Comparison between the front, center, and back measured widths for the 1.0" part using citric not misted 2Dir. 900°C variables. The points represent the average width,. Error bars show the standard deviation of the measurements divided by the sq. root of the number of measurements, 15 measurements.

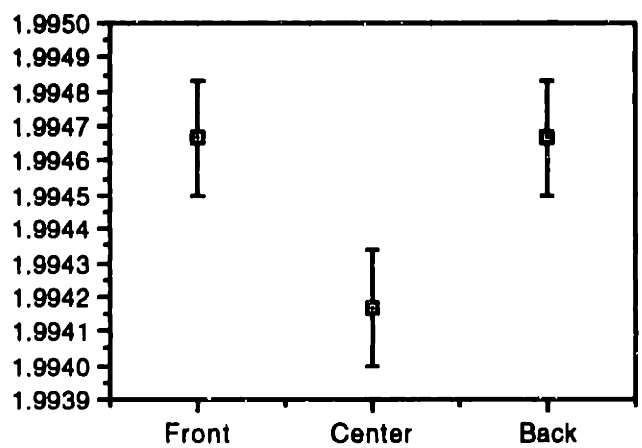

Figure 4.8: Experiment 2 in table 2.2: Comparison between the front, center, and back measured widths for the 2.0" part using citric not misted 2Dir. 900°C variables, The points represent the average width. Error bars show the standard deviation of the measurements divided by the sq. root of the number of measurements, 15 measurements.

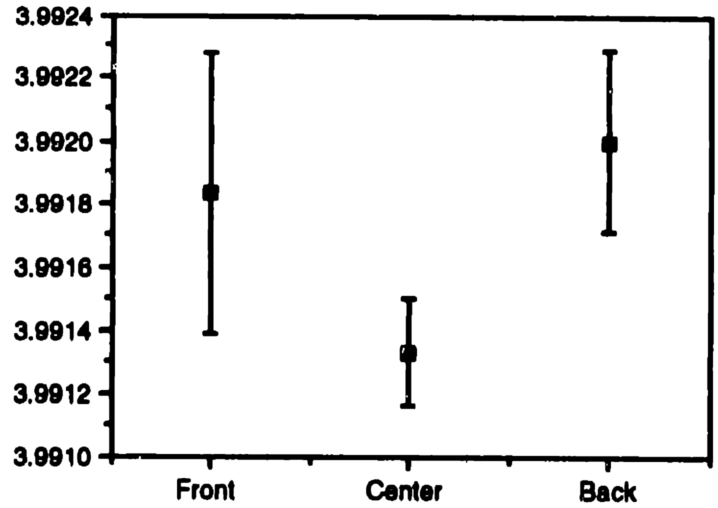

Figure 4.9: Experiment 2in table 2.2: Comparison between the front, center, and back measured widths for the 4.0" part using citric not misted 2Dir. 900°C variables, The points represent the average width. Error bars show the standard deviation of the measurements divided by the sq. root of the number of measurements, 15 measurements.

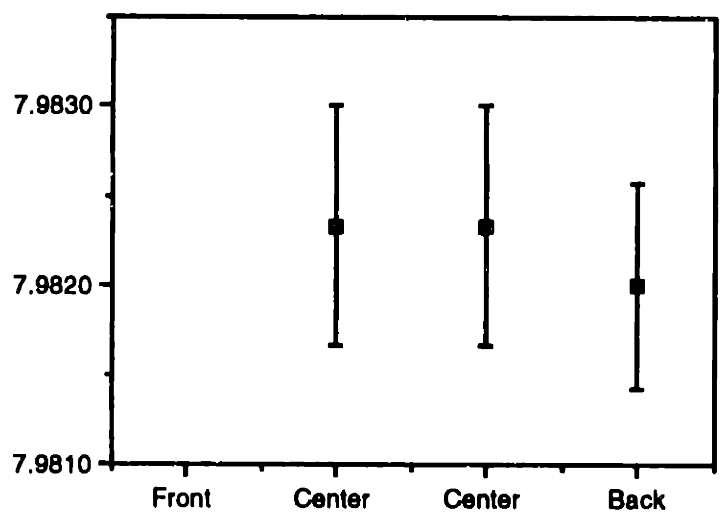

Figure 4.10: Experiment 2in table 2.2: Comparison between the front, center, and back measured widths for the 8.0" part using citric not misted 2Dir. 900°C variables, The points represent the average width. Error bars show the standard deviation of the measurements divided by the sq. root of the number of measurements, 15 measurements.

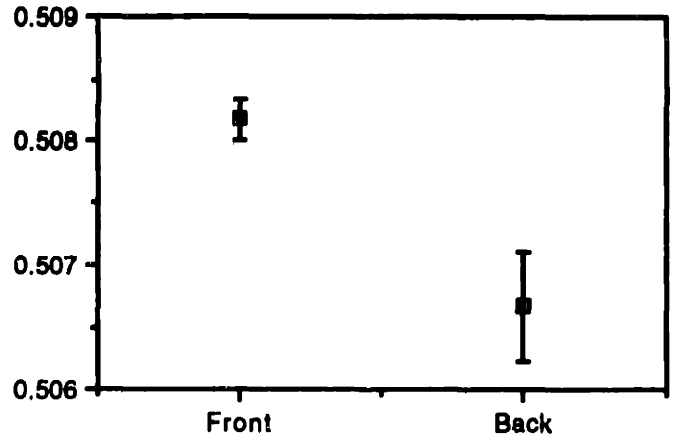

Figure 4.11: Experiment 3in table 2.2:. Comparison between the front and back measured widths for the 0.5" part using citric misted 1Dir. 900'C variables, The points represent the average width. Error bars show the standard deviation of the measurements divided by the sq. root of the number of measurements, 15 measurements.

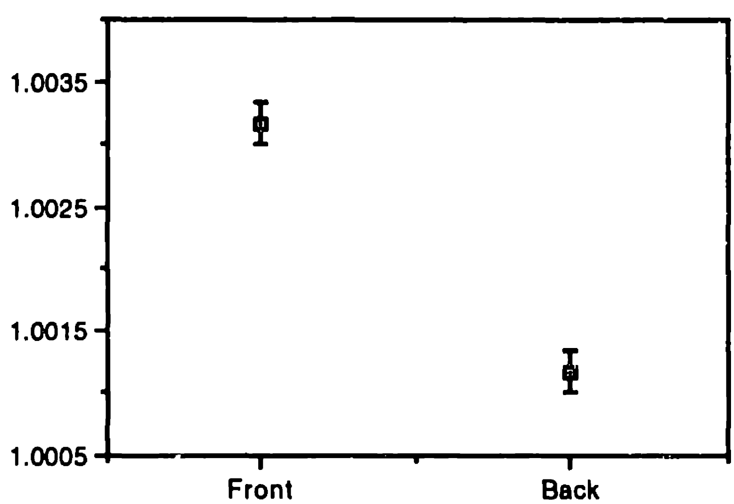

Figure 4.12: Experiment 3 in table 2.2.: Comparison between the front and back measured widths for the 1.0" part using citric misted 1Dir. 900'C variables, The p nts represent the average width. Error bars show the standard deviation of the measurements divided by the sq. root of the number of measurements, 15 measurements.

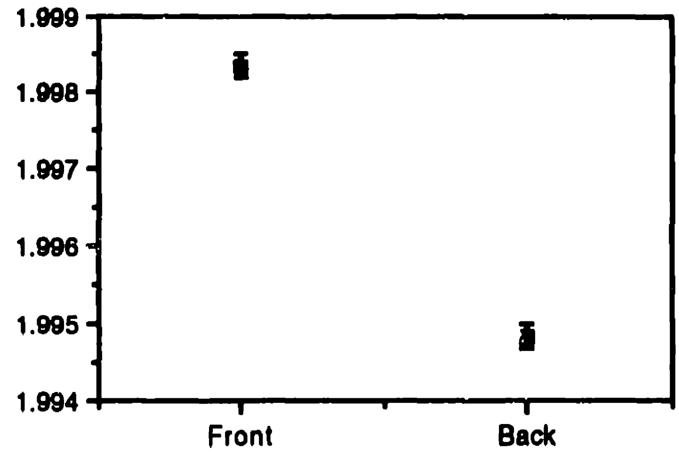

Figure 4.13: Experiment 3in table 2.2.: Comparison between the front and back measured widths for the 2.0" part using citric misted 1Dir. 900°C variables, The points represent the average width. Error bars show the standard deviation of the measurements divided by the sq. root of the number of measurements, 15 measurements.

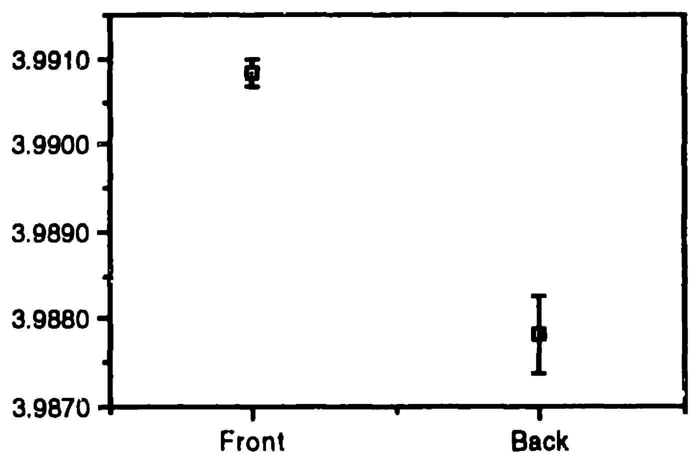

Figure 4.14: Experiment 3 in table 2.2.: Comparison between the front and back measured widths for the 4.0" part using citric misted 1Dir. 900°C variables. The points represents the average width. Error bars show the standard deviation of the measurements divided by the sq. root of the number of measurements, 15 measurements.

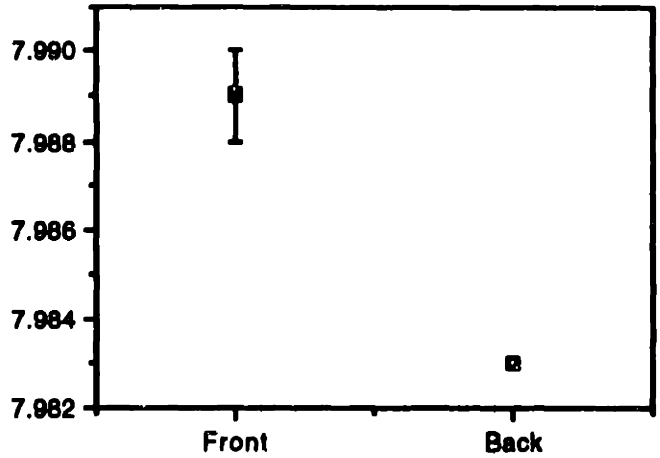

Figure 4.15: Experiment 3in table 2.2: Comparison between the front and back measured widths for the 8.0" part using citric misted 1Dir. 900°C variables. The points represent the average width. Error bars show the standard deviation of the measurements divided by the sq. root of the number of measurements, 15 measurements.

As noted there is a 75 % confidence, using ANOVA method, in saying that back parts shrink more than front parts in the citric misted 2 Dir 900°C experiment. On the other hand, there is no conclusion about the shrinkage difference between the front and the back parts in the citric not misted 2 Dir. 900°C experiment. The difference between the front and back for the citric, misted 1 direction 900°C parts is very noticeable and increases as the part's width increases in the fast axis. There is a 100% confidence in saying that the front bars shrink less than the back bars. Table 4.1 shows the difference between the front and the back for the 0.5", 1.0", 2.0", 4.0", and 8.0" bars.

Table 4.1: The difference between the front and back parts for citric, misted, 1Dir.900°C parts

Part	**0.5"**	**1.0"**	**2.0"**	**4.0"**	**8.0"**
Front-Back	0.0015"	0.002"	0.0035"	0.003"	0.006"

- For a better fit, some graphs could have been polynomial of the second degree fit so that the curve would pass through the error bars of the measurements. The non linear behavior of the results is due to what is being modeled as frictional force. Hypothetically there is a frictional force between the printed line as it is being deposited and the adjacent loose powder . The frictional force magnitude depend on the dimension of the part itself in a non linear fashion and on its shape. Small parts tend to have a higher shrinkage than larger ones because the friction force is small, on the other hand large parts shrink less since the magnitude of the frictional force is large and prevent their shrinkage.
- The frictional force hypothesis is more confirmed since Jain Charnnmmarong had discovered recently that 80% of the parts shrinkage occurs in the drying stage before firing. His findings indicates that dimensional error occurs mainly when the part is being printed, supporting the friction hypothesis since it is the only major factor before firing.

4.2 Conclusions for the Drag Error Effect

The hypothetical idea that there is a drag force on the first drop is partially right. There is a drag force but not on the first drop of the binder stream as was assumed. It is on all the binder drops. This conclusion is reached because there is **no** significant shift between the last drops of line set A and the first drops of line set B. The reason for not detecting the shift is because the reference frame that was chosen , the last drops of line set A which are suppose to fall exactly at position 1000 μm, itself was shifted by the drag force. All the lines were shifted and the technique chosen for printing lines for sets A&B was not appropriate. Nonetheless, this technique proved at least that the air drag acts continuously on all the binder drops.

Since the drag force tends to shift all printed lines, one could conclude that, the part's dimension in the fast axis is **not** affected by it. The drag force simply acts as an external fixed parameter that carries the whole line from the intended location to another, but the **length** of the line is not affected.

5 Recommendations

Understanding the control of dimensions for printed ceramic parts using the 3D printing machine is a topic of importance to the accuracy of the parts for their industrial usage. This research has made several findings in the area of the dimensional errors. The following are recommendations for future research.

- The graphs that represent dimensional deviations, figures 3.1 to 3.14, could be usefully used to compare dimensional errors of different powders and different variables.
- Another important issue that has to be further addressed is the full use of an orthogonal experimental process. Because of the constrains of time and the expense of 3D printing, only part of the orthogonal process was conducted. A continuum of the experiments for different variable settings is desirable.
- Even though calipers were the best measuring tool when the experiments were done, their usage are not ultimately the best way for a dimensionally dependent research. An excellent alternative would be a coordinate measuring machine, CM, because of its high accuracy.
- The experiments carried out concentrated on dimensional control in the fast and slow axes of printing. To fully understand the dimensional errors in the 3D process, one should print bars of different heights in the Z-axis and then perform control of dimensions on those parts. It may be the case that the errors' magnitudes in the fast and slow axes change for different part heights.
- In order to understand the effect of frictional force on printed parts, one should print parts which have lengths less than 0.7441", measure their dimensions, and plot graphs, to see what kind of fit goes through them and to see wither or not the frictional force has a different values for small parts.
- Another recommendation about the frictional force is to find wither or not the geometry of the parts have an affect on the frictional force. Since only rectangular

parts were printed, a T shape parts would be suggested to see if there is a difference in shrinkage.

- In order to reduce the shrinkage, a better understanding of the frictional force could be the first step.
- There are two conclusion for the drag force effect. The first is that the drag force affects all the binder stream drops. The second is that the drag force shifts the line the intended location to another. However, the magnitude of the resulting shift is not yet determined. A second technique that would make drag force effects fully understanding should be found.

Appendix A: Data of the Measurements in the Slow Axis

A.1 Data for experiment 1: Citric misted 2Dir. 750°C parts.

Measured Length "in"	Deviation of Length "in"
0.38150	0.00950
0.38250	0.01050
0.38200	0.01000
0.38250	0.01050
0.38200	0.01000
0.75150	0.00740
0.75200	0.00790
0.75150	0.00740
0.75150	0.00740
0.75200	0.00790
2.00350	0.00550
2.00300	0.00500
2.00300	0.00500
2.00350	0.00550
2.00250	0.00450
3.99750	0.00140
3.99700	0.0009

A2 Data For Experiment 2 : Citric not misted 2Dir. 750°C parts.

Measured Length	Deviation of Length
0.38000	0.00800
0.37900	0.00700
0.38100	0.00900
0.38000	0.00800
0.38000	0.00800
0.38100	0.00900
0.38050	0.00850
0.75250	0.00840
0.75250	0.00840
0.75200	0.00790
0.75300	0.00890
0.75200	0.00790
0.75150	0.00740
0.75250	0.00840
0.75200	0.00790
0.75150	0.00740
0.75250	0.00840
0.75200	0.00790
0.75200	0.00790
0.75250	0.00840
0.75250	0.00840
0.75250	0.00840
2.00400	0.00600
2.00350	0.00550
2.00350	0.00550
2.00400	0.00600
2.00300	0.00500
2.00300	0.00500
2.00300	0.00500
2.00300	0.00500
2.00250	0.00450
2.00300	0.00500
2.00300	0.00500
2.00250	0.00450
2.00300	0.00500
2.00300	0.00500
2.00300	0.00500
3.99800	0.00190
3.99700	0.00090
3.99950	0.00340
3.99650	0.00040
3.99700	0.00090
3.99700	0.00090
3.99800	0.00190
3.99800	0.00190
3.99950	0.00340
4.00000	0.00390
3.99800	0.00190

A.3 Data for experiment 3: Non citric misted 2Dir. 750°C parts.

Measured Length "in"	Deviation of Length "in"
0.381500	0.009500
0.381500	0.009500
0.380500	0.008500
0.381500	0.009500
0.381500	0.009500
0.381500	0.009500
0.381000	0.009000
0.381000	0.009000
0.380500	0.008500
0.381000	0.009000
0.380500	0.008500
0.380500	0.008500
0.381500	0.009500
0.380500	0.008500
0.380500	0.008500
0.752000	0.007900
0.752500	0.008400
0.751500	0.007400
0.751500	0.007400
0.753000	0.008900
0.752500	0.008400
0.753500	0.009400
0.753000	0.008900
0.753000	0.008900
0.753000	0.008900
0.752500	0.008400
0.753000	0.008900
0.753500	0.009400
0.753500	0.009400
0.753000	0.008900
2.005000	0.007000
2.005000	0.007000
2.005000	0.007000
2.004500	0.006500
2.004000	0.006000
2.004000	0.006000
2.005500	0.007500
2.005000	0.007000
2.005000	0.007000
2.006000	0.008000
2.005500	0.007500
2.005000	0.007000
4.001000	0.004900
4.001000	0.004900
4.003000	0.006900

A.4 Data for Experiment 4: Non citric not misted 2 Dir. 750° C parts.

Measured Length "in"	Deviation of Length "in"	Measured Length "in"	Deviation Of Length "in"
0.38300	0.01100	2.00600	0.00800
0.38300	0.01100	2.00600	0.00800
0.38400	0.01200	2.00600	0.00800
0.38300	0.01100	2.00550	0.00750
0.38350	0.01150	2.00600	0.00800
0.38300	0.01100	2.00600	0.00800
0.38300	0.01100	2.00600	0.00800
0.38400	0.01200	2.00550	0.00750
0.38350	0.01150	2.00550	0.00750
0.38300	0.01100	2.00500	0.00700
0.38300	0.01100	2.00550	0.00750
0.38300	0.01100	2.00550	0.00750
0.75400	0.00990	2.00500	0.00700
0.75500	0.01090	2.00600	0.00800
0.75400	0.00990	2.00500	0.00700
0.75400	0.00990	4.00100	0.00490
0.75300	0.00890	4.00000	0.00390
0.75400	0.00990	4.00050	0.00440
0.75450	0.01040	4.00050	0.00440
0.75450	0.01040	4.00050	0.00440
0.75350	0.00894	4.00050	0.00440
0.75350	0.00894	4.00050	0.00440
0.75350	0.00894	4.00000	0.00390
0.75450	0.01040	4.00000	0.00390
0.75350	0.00894	4.00000	0.00390
0.75300	0.00890	4.00100	0.00490
0.75300	0.00890	4.00050	0.00440
2.00600	0.00800	4.00000	0.00390
2.00600	0.00800	4.00050	0.00440
2.00600	0.00800	3.99950	0.00340

A.5 Data for experiment 5: Citric misted 2Dir. 900°C parts.

Measured Length "in"	Deviation of Length "in"
0.38100	0.00900
0.38300	0.01100
0.38250	0.01050
0.38200	0.01000
0.38250	0.01050
0.38200	0.01000
0.38150	0.00950
0.38250	0.01050
0.38150	0.00950
0.38200	0.01000
0.38200	0.01000
0.38200	0.01000
0.38100	0.00900
0.38100	0.00900
0.38100	0.00900
0.75050	0.00640
0.75000	0.00590
0.75100	0.00690
0.75100	0.00690
0.75100	0.00690
0.75100	0.00690
0.75100	0.00690
0.75100	0.00690
0.75100	0.00690
0.75100	0.00690
0.75100	0.00690
0.75100	0.00690
0.75100	0.00690
0.74950	0.00540
0.74950	0.00540
2.00200	0.00400
2.00250	0.00450
2.00250	0.00450
2.00200	0.00400
2.00200	0.00400
2.00200	0.00400
2.00250	0.00450
2.00300	0.00500
2.00300	0.00500
2.00150	0.00350
2.00200	0.00400

A.6 Data for experiment 6: Citric not misted 2Dir. 900°C parts.

Measured Length "in"	Deviation of Length "in"
0.75200	0.00790
0.75150	0.00740
0.75150	0.00740
0.75150	0.00740
0.75150	0.00740
0.75150	0.00740
2.00250	0.00450
2.00300	0.00500
2.00200	0.00400
2.00250	0.00450
2.00250	0.00450
2.00200	0.00400
3.99650	0.00040
3.99550	-0.00060
3.99450	-0.00160
3.99500	-0.00110
3.99400	-0.00210
3.99400	-0.00210

Appendix B: Data of the Measurements in the Fast Axis

B.1 Data for experiment 1: Citric misted 2Dir. 900° C parts

Front Data	Deviation	Back Data	Deviation
0.50600	0.00600	0.505	0.005
0.50550	0.00550	0.504	0.004
0.50550	0.00550	0.504	0.004
1.00300	0.00300	1.005	0.005
1.00150	0.00150	1.005	0.005
1.00200	0.00200	1.000	-0.000
1.99700	-0.00300	1.996	-0.005
1.99700	-0.00300	1.996	-0.004
1.99600	-0.00400	1.995	-0.005
3.98950	-0.01050	3.989	-0.010
3.98850	-0.01150	3.989	-0.011
3.98800	-0.01200	3.988	-0.011
7.98200	-0.01800	7.980	-0.020
7.98000	-0.02000	7.980	-0.020
7.98100	-0.01900	7.980	-0.020

B.2 Data for experiment 2: Citric not misted 2Dir. 900°C parts.

Front Data	Deviation	Center Data	Deviation	Back Data	Deviation
0.502000	0.002000	0.502000	0.002000	0.502000	0.002000
0.501500	0.001000	0.501500	0.001500	0.502000	0.002000
0.502000	0.002000	0.501500	0.001500	0.501500	0.001500
0.999000	-0.001000	0.999000	-0.001000	0.999500	-0.000500
0.998000	-0.002000	0.998500	-0.001500	0.998500	-0.001500
0.998000	-0.002000	0.998500	-0.001500	0.998500	-0.001500
1.994500	-0.005500	1.994000	-0.006000	1.994500	-0.005500
1.994500	-0.005500	1.994500	-0.005500	1.994500	-0.005500
1.995000	-0.005000	1.994000	-0.006000	1.995000	-0.005000
3.992500	-0.007500	3.991500	-0.008500	3.992500	-0.007500
3.991000	-0.009000	3.991500	-0.008500	3.991500	-0.008500
3.992000	-0.008000	3.991000	-0.009000	3.992000	-0.008000
7.984000	-0.016000	7.983000	-0.017000	7.983000	-0.017000
7.983000	-0.017000	7.981000	-0.019000	7.981000	-0.019000
7.984000	-0.016000	7.983000	-0.017000	7.983000	-0.017000
7.983000	-0.017000	7.983000	-0.017000	7.981000	-0.019000
7.981000	-0.019000	7.981000	-0.019000	7.982000	-0.018000
7.983000	-0.017000	7.983000	-0.017000	7.983000	-0.017000

B.3 Data for experiment 3: Citric misted 1Dir. 900°C parts.

Front Data	Deviation	Back Data	Deviation
7.99000	-0.01000	7.98300	-0.01700
7.98700	-0.01300	7.98300	-0.01700
0.50900	0.00800	0.50700	0.00700
0.50800	0.00800	0.50600	0.00600
0.50800	0.00800	0.50600	0.00700
1.00300	0.00300	1.00100	0.00100
1.00300	0.00300	1.00100	0.00100
1.00300	0.00300	1.00100	0.00100
1.99900	-0.00100	1.99500	-0.00500
1.99800	-0.00200	1.99500	-0.00500
1.99900	-0.00100	1.99400	-0.00500
3.99100	-0.00900	3.98800	-0.01200
3.99100	-0.00900	3.98700	-0.01300
3.99100	-0.01000	3.98800	-0.01100